The EMBO Journal (2006) 25, 4175–4186 | © 2006 European Molecular Biology Organization | All Rights Reserved 0261-4189/06
www.embojournal.org

THE EMBO JOURNAL

Secretion of L-glutamate from osteoclasts through transcytosis

Riyo Morimoto[1,6], Shunsuke Uehara[1,6], Shouki Yatsushiro[1], Narinobu Juge[1], Zhaolin Hua[2], Shigenori Senoh[1], Noriko Echigo[1], Mitsuko Hayashi[1], Toshihide Mizoguchi[3], Tadashi Ninomiya[3], Nobuyuki Udagawa[4], Hiroshi Omote[1], Akitsugu Yamamoto[5], Robert H Edwards[2] and Yoshinori Moriyama[1,*]

[1]Laboratory of Membrane Biochemistry, Okayama University Graduate School of Medicine, Dentistry, and Pharmaceutical Sciences, Okayama, Japan, [2]Departments of Neurology and Physiology, Graduate Programs in Neuroscience and Cell Biology, University of California San Francisco School of Medicine, CA, USA, [3]Institute for Oral Science, Matsumoto Dental University, Shiojiri, Japan, [4]Department of Biochemistry, Matsumoto Dental University, Shiojiri, Japan and [5]Department of Cell Biology, Nagahama Institute of Bioscience and Technology, Nagahama, Japan

Osteoclasts are involved in the catabolism of the bone matrix and eliminate the resulting degradation products through transcytosis, but the molecular mechanism and regulation of transcytosis remain poorly understood. Upon differentiation, osteoclasts express vesicular glutamate transporter 1 (VGLUT1), which is essential for vesicular storage and subsequent exocytosis of glutamate in neurons. VGLUT1 is localized in transcytotic vesicles and accumulates L-glutamate. Osteoclasts secrete L-glutamate and the bone degradation products upon stimulation with KCl or ATP in a Ca^{2+}-dependent manner. KCl- and ATP-dependent secretion of L-glutamate was absent in osteoclasts prepared from VGLUT1$^{-/-}$ knockout mice. Osteoclasts express mGluR8, a class III metabotropic glutamate receptor. Its stimulation by a specific agonist inhibits secretion of L-glutamate and bone degradation products, whereas its suppression by a specific antagonist stimulates bone resorption. Finally, it was found that VGLUT1$^{-/-}$ mice develop osteoporosis. Thus, in bone-resorbing osteoclasts, L-glutamate and bone degradation products are secreted through transcytosis and the released L-glutamate is involved in autoregulation of transcytosis. Glutamate signaling may play an important role in the bone homeostasis.

The EMBO Journal (2006) **25,** 4175–4186. doi:10.1038/sj.emboj.7601317; Published online 7 September 2006
Subject Categories: membranes & transport; signal transduction
Keywords: bone resorption; osteoclast; osteoporosis; transcytosis; vesicular glutamate transporter

*Corresponding author. Department of Membrane Biochemistry, Graduate School of Medicine, Dentistry, and Pharmaceutical Sciences, Okayama University, Okayama 700-8530, Japan.
Tel.: +81 86 251 7933/7934; Fax: +81 86 251 7935;
E-mail: moriyama@pheasant.pharm.okayama-u.ac.jp
[6]These authors contributed equally to this work

Received: 28 October 2005; accepted: 8 August 2006; published online: 7 September 2006

Introduction

Bone resorption is an essential component of bone remodeling during the development, growth and turnover of bone. An imbalance contributes to the pathogenesis as well as the etiology of metabolic diseases such as osteoporosis and osteopetrosis (Eriksen, 1986; Rodan and Martin, 2000; Boyle *et al*, 2003). Osteoclasts are multinuclear cells originating from monocyte/macrophage lineage cells and are primarily responsible for bone resorption (Baron *et al*, 1994; Blair, 1998; Väänänen *et al*, 2000). During the resorption process, osteoclasts are highly polarized, form tightly sealed compartments (i.e., resorption lacunae) on the bone surface and secrete protons, chloride anions and proteases through the ruffled border, resulting in the degradation of the bone matrix. To transport a large amount of degradation products, osteoclasts develop an inwardly polarized membrane traffic called transcytosis: inorganic and organic degradation products and cathepsin K are taken up at the ruffled border through endocytosis, packaged into transcytotic vesicles, transported along microtubules to the basolateral plasma membrane and then secreted through exocytosis (Nesbitt and Horton, 1997; Salo *et al*, 1997; Mulari *et al*, 2003). The overall secretory processes are believed to be highly organized and coordinated with other bone functions, although the mechanisms and regulation of transcytosis remain poorly understood.

L-Glutamate, an excitatory neurotransmitter of the central nervous system, acts as an intercellular messenger in peripheral non-neuronal cells, in which L-glutamate is stored in secretory vesicles and secreted through regulated exocytosis and, thus, enables intercellular chemical transmission in a paracrine or autocrine manner (Moriyama and Yamamoto, 2004). Although there is evidence for L-glutamate signaling in bone, its physiological significance has not been established (Serre *et al*, 1999; Bhangu *et al*, 2001; Hinoi *et al*, 2001; Skerry and Taylor, 2001; Mason, 2004). Bone cells express the GLAST-type Na^+-dependent plasma membrane transporter, which terminates L-glutamate signals (Skerry and Taylor, 2001; Mason, 2004). Bone cells also express various functional glutamate receptors, and their stimulation affects the functions of osteoblasts and osteoclasts (Skerry and Taylor, 2001; Mason, 2004). However, it is still unresolved where, when and how L-glutamate appears as an intercellular messenger in bone. Although L-glutamate has been suggested to originate from L-glutamate-containing nerve terminals (Serre *et al*, 1999) or osteoblasts (Bhangu *et al*, 2001; Hinoi *et al*, 2002), secretion of L-glutamate from nerve terminals has not been detected. Furthermore, the mode of secretion of L-glutamate from osteoblasts differs from that of the exocytosis of L-glutamate in CNS or endocrine cells.

Vesicular glutamate transporter (VGLUT) plays an essential role in L-glutamate signaling through vesicular storage of L-glutamate (Fremeau *et al*, 2004a;Moriyama and Yamamoto, 2004). There are three isoforms of VGLUT: VGLUT1, VGLUT2

and VGLUT3. VGLUT is a potential marker for the sites of L-glutamate signaling and can help reveal details of the mode of glutamate signaling in the body (Moriyama and Yamamoto, 2004).

In the present study, we examined the expression and localization of VGLUT in bone tissue to determine how L-glutamate becomes an intercellular messenger. We found an unexpected link between L-glutamate signaling and bone resorption. We show that (1) mature osteoclasts possess VGLUT1-containing transcytotic vesicles and thus secrete L-glutamate and bone degradation products through transcytosis, (2) this glutamate signaling is involved in autoregulation of transcytosis and (3) impairment of the glutamate signaling stimulates bone resorption and may contribute to the development of osteoporosis.

Results

VGLUT1 was expressed in osteoclasts

RT–PCR analysis demonstrated that osteoclasts derived from bone marrow cells contained mRNA encoding VGLUT1 and that other types of bone cells including primary osteoblasts, stroma cells and clonal bone cells did not express this mRNA (Figure 1A). Neither VGLUT2 nor VGLUT3 was expressed in any of the bone cells analyzed (Figure 1B). Northern blot analysis revealed mRNA of VGLUT1 in mature osteoclasts but not in undifferentiated cells (Figure 1C). Upon stimulation with RANKL, a receptor activator of the nuclear factor κB ligand, murine macrophage RAW264.7 cells can differentiate into osteoclasts (Toyomura *et al*, 2003) that then express the VGLUT1 gene (Figure 1A and C). These results indicate that the VGLUT1 gene was specifically expressed in osteoclasts during differentiation and that expression of the VGLUT2 and VGLUT3 genes in bone cells was negligible or below the detection limit of our assay.

Immunoblotting with VGLUT1 antibodies revealed that an immunoreactive polypeptide with an apparent molecular mass similar to that of VGLUT1 (~62 kDa) appeared in RAW264.7 cells upon treatment of RANKL, whereas expression of the housekeeping vacuolar H^+-ATPase (V-ATPase) subunit was the same before and after differentiation (Figure 1D).

Inducible expression of VGLUT1 immunoreactivity in RAW264.7 cells treated with RANKL was confirmed by immunohistochemistry: VGLUT1 immunoreactivity appeared 3 days after induction and reached a steady-state level after 7 days (Figure 1E). The presence of VGLUT1 immunoreactivity in tartrate-resistant acid phosphatase (TRAP)-positive osteoclasts was confirmed in the femurs of VGLUT1$^{+/+}$ (wild type) mice but not in those of VGLUT1$^{-/-}$ mice (Figure 1F). Essentially the same results were obtained in osteoclasts prepared from VGLUT1$^{+/+}$ (wild type) mice but not in those of VGLUT1$^{-/-}$ mice (Supplementary Figure S1). Overall, these results demonstrate that VGLUT1 appeared in osteoclasts during osteoclastogenesis.

VGLUT1 was associated with transcytotic vesicles

To identify VGLUT1-containing organelles, we performed immunohistochemical analyses. After culturing on bone, an actin ring was observed, indicating the site of bone digestion (Figure 2A). The VGLUT1 immunoreactivity exhibited a punctated distribution throughout the cells and was especially abundant in the basolateral region, but less in the ruffled border region (Figure 2A and B). VGLUT1 was roughly co-localized with microtubules but not with actin (Figure 2A and B). VGLUT1 did not seem to be co-localized with Lamp2, TGN38, GM130 or transferrin receptor (TfR), which are markers for lysosomes, the Golgi apparatus, endosomes and recycling vesicles, respectively (Supplementary Figure S2), but rather was partially co-localized with lysobisphosphatidic acid, a phospholipid abundant in late endosomes (Figure 2C), and cathepsin K (Figure 2D), both of which are associated with the transcytotic pathway after endocytosis (Vääräniemi *et al*, 2004). Furthermore, VGLUT1 immunoreactivity was, in part, co-localized with the internalized fluorescent bone degradation products (Figure 2E). These results suggest that VGLUT1 was associated with the vesicles involved in the transcytotic pathway, such as transcytotic vesicles.

VGLUT1-containing vesicles were identified through double immunoelectron microscopy. Consistent with the immunohistochemical observations made above, there were at least three types of vesicles associated with immunogold particles specific for VGLUT1 and bone degradation products: many clear vesicles with an average diameter of ~300 nm in which VGLUT1 was present but in which immunoreactivity for bone degradation products was not detected (Figure 3A); larger vesicles located near basolateral regions that contained many VGLUT1 immunogold particles and some particles for bone degradation products (Figure 3B); and larger vesicles located near the ruffled border membrane that contained many immunogold particles for bone degradation products and a few immunogold particles for VGLUT1 (Figure 3C). We concluded that a population of VGLUT1 was associated with the transcytotic vesicles that contain bone degradation products. The dynamics of these vesicles during transcytosis is discussed later.

VGLUT1 in osteoclasts was functional

We then determined whether VGLUT1-containing vesicles accumulate L-glutamate. Generally, V-ATPase supplies the driving force for the vesicular storage of L-glutamate (Maycox *et al*, 1990; Moriyama and Yamamoto, 2004). We prepared membrane vesicles from RAW264.7 cells treated with or without RANKL. Upon the addition of ATP, a substantial amount of L-glutamate was taken up by vesicles isolated from RAW264.7 cells treated with RANKL and much less was taken up by those isolated from undifferentiated control RAW264.7 cells (Figure 4A). The ATP-dependent L-glutamate uptake was blocked by carbonyl cyanide-*m*-chlorophenylhydrazone (CCCP, a proton conductor), bafilomycin A1 (V-ATPase inhibitor; Bowman *et al*, 1988) and Evans blue (an inhibitor of VGLUT; Roseth *et al*, 1998), but not affected by 10 mM D,L-aspartate (Figure 4B). A low concentration of Cl^- (4 mM) was required for L-glutamate uptake; in the absence of Cl^-, the uptake decreased to background level (Figure 4B). The results were fully consistent with the properties of VGLUT-mediated L-glutamate transport (Moriyama and Yamamoto, 2004), and demonstrated VGLUT1-dependent vesicular storage of L-glutamate in bone-resorbing RAW264.7 cells treated with RANKL.

Osteoclasts secreted L-glutamate through transcytosis

Do osteoclasts secrete L-glutamate? As the exocytosis of L-glutamate is usually driven by membrane depolarization,

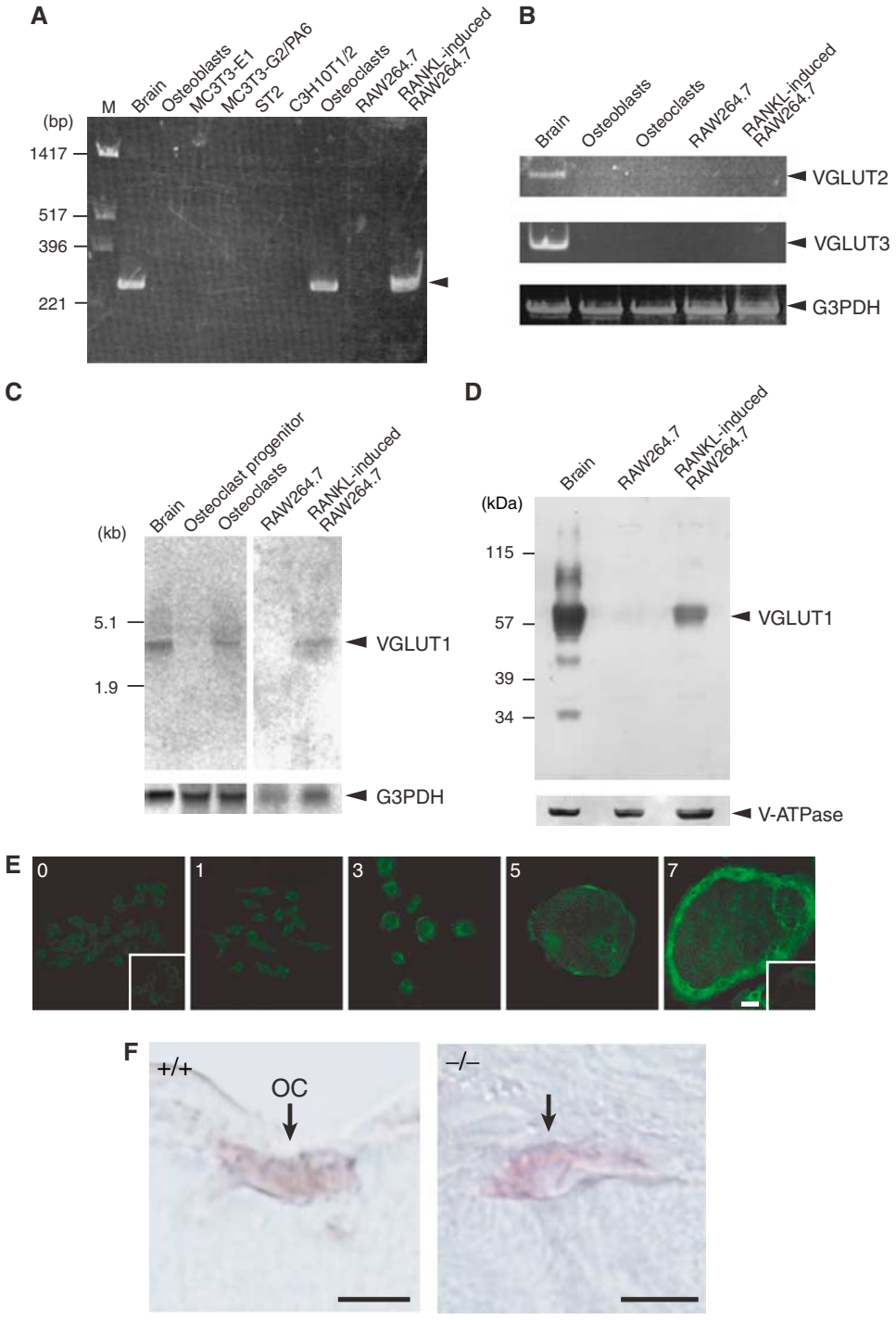

Figure 1 Inducible expression of VGLUT1 in osteoclasts. (**A**) RT–PCR analysis of brain, osteoblasts, MC3T3-E1 (clonal osteoblasts), MC3T3-G2/PA6 (clonal stroma cell line from calvariae), ST2 (clonal stroma cell line from bone marrow), C3H10T1/2 (clonal fibroblast cell line), osteoclasts, RAW264.7 macrophages and RAW264.7 cells treated with RANKL. The arrowhead indicates the VGLUT1 transcript. (**B**) VGLUT2 and VGLUT3 genes were not detectable in bone cells. Results of RT–PCR analysis of total cellular RNA are shown. Expression of G3PDH gene is also shown as a control. (**C**) Northern blotting revealing expression of the VGLUT1 gene in mature osteoclasts and RAW264.7 cells treated with RANKL. The G3PDH transcript, as a loading control, is also shown (lower panel). (**D**) Western blotting reveals the presence of VGLUT1 in RAW264.7 cells treated with RANKL. The presence of V-ATPase subunit *A* on the same blot is also shown. (**E**) RAW264.7 cells were cultured in the presence of RANKL for the indicated incubation periods (days) and the expression of VGLUT1 during osteoclastogenesis was observed by immunohistochemistry. Negative control with control IgG is also shown in insets. Bar = 10 μm. (**F**) Osteoclasts (OC) in the femora of VGLUT1$^{+/+}$ (wild type) mice visualized by TRAP staining (red) contain VGLUT1, which was visualized by the horseradish peroxidase-diaminobenzidine (HRP-DAB) method (charcoal). No VGLUT1 immunoreactivity was seen in osteoclasts from VGLUT1$^{-/-}$ mice. Bar = 10 μm.

we measured the L-glutamate present in the medium after depolarization of osteoclasts with KCl. KCl at 50 mM depolarizes bone-resorbing osteoclasts through a voltage-gated K^+ channel (Kajiya *et al*, 2003). We found that KCl stimulated the secretion of L-glutamate from RAW264.7 cells treated with RANKL and to a lesser extent from undifferen-

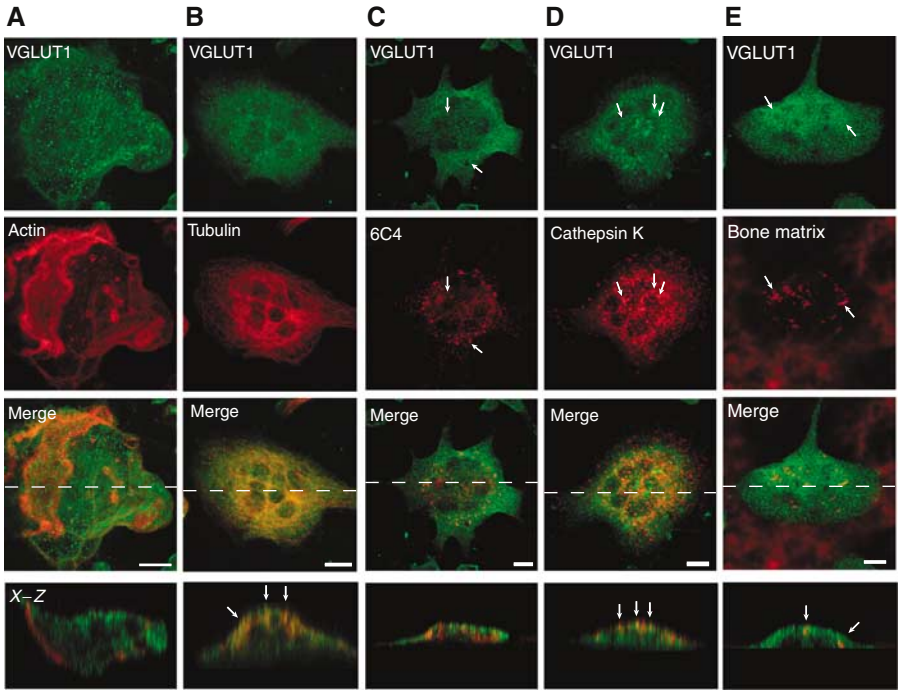

Figure 2 Immunohistochemical localization of VGLUT1 in bone-resorbing osteoclasts. Osteoclasts were grown on pieces of bone. Localization of VGLUT1 was examined by double-labeling immunofluorescence microscopy. The staining pairs were as follows: VGLUT1 and actin (**A**), VGLUT1 and tubulin (**B**), VGLUT1 and lysobisphosphatidic acid (6C4) (**C**), VGLUT1 and cathepsin K (**D**) and VGLUT1 and fluorescent bone degradation products (**E**). The immunological localization was observed under a confocal microscope. A horizontal view of a merged picture is also shown. Bar = 10 μm.

tiated control cells (Figure 5A). The KCl-evoked L-glutamate secretion was dependent on extracellular Ca^{2+} and temperature: depletion of Ca^{2+} by treatment with EGTA-AM inhibited the secretion by 80% and low temperature (24°C) abolished the secretion (Figure 5B). Consistent with its effect on the vesicular storage of L-glutamate (Figure 4), bafilomycin A1 decreased L-glutamate secretion (Figure 5B). These properties are similar to those reported for the regulated exocytosis of L-glutamate by neurons and endocrine cells (Moriyama and Yamamoto, 2004).

As a population of VGLUT1 is associated with transcytotic vesicles, secretion of L-glutamate may accompany, at least in part, the secretion of bone degradation products. As expected, KCl stimulated secretion of fluorescent bone degradation products (Figure 5C). The secretion also required extracellular Ca^{2+} and was sensitive to temperature and bafilomycin A1 (Figure 5C). Bafilomycin A1 is also known to inhibit transcytosis (Palokangas *et al*, 1997; Stenbeck and Horton, 2004). Furthermore, nocodazole, a reagent that dissociates microtubules and, through this, inhibits transcytosis (Stenbeck and Horton, 2004), inhibited the secretion of both L-glutamate and bone degradation products to a similar extent (Figure 5B and C). These results support the idea that L-glutamate was co-secreted with bone degradation products through transcytosis.

It is important to ask what kinds of stimuli trigger transcytosis under physiological conditions. We found that ATP at 1 mM stimulated the secretion of both L-glutamate (Figure 5D) and bone degradation products (Figure 5E), and was blocked by pyridoxalphosphate-6-azophenyl-2′-4′-disulfonic acid (PPADS), a selective antagonist of ionotropic purinergic receptors (Ralevic and Burnstock, 1998). As ATP is secreted from osteoblasts upon mechanical stimulation and depolarizes osteoclasts so as to increase the cytosolic concentration of Ca^{2+} via ionotropic purinergic receptors (Naemsch *et al*, 2001; Romanello *et al*, 2001), the results suggest that ATP was one of the physiological stimuli for secretion of L-glutamate and bone degradation products.

L-Glutamate secretion from osteoclasts from VGLUT1$^{-/-}$ mice

We then assessed L-glutamate secretion from osteoclasts prepared from VGLUT1$^{-/-}$ mice. The number and morphology of osteoclasts from VGLUT1$^{+/-}$ heterozygotes and VGLUT1$^{-/-}$ homozygotes were apparently comparable to those of wild-type osteoclasts. As shown in Figure 6A and B, KCl stimulated the secretion of L-glutamate in osteoclasts from wild-type and heterozygotic mice by a factor of ~2. The KCl-evoked secretion of L-glutamate was not observed in the case of osteoclasts from VGLUT1$^{-/-}$ homozygotes (Figure 6C). Essentially the same results were obtained when the L-glutamate secretion was evoked by ATP (Figure 6D). In contrast to the L-glutamate secretion, KCl-mediated secretion of bone degradation products was not altered in osteoclasts of all three mice genotypes (Figure 6E).

mGluR8-mediated autoregulation of transcytosis

Subsequently, we investigated the role of the released L-glutamate. As L-glutamate signaling in peripheral tissues usually involves an autoregulatory mechanism by way of metabotropic receptors (Yamada *et al*, 1998; Uehara *et al*, 2004), we investigated whether mGluRs are expressed in osteoclasts, and if so, whether they regulate transcytosis.

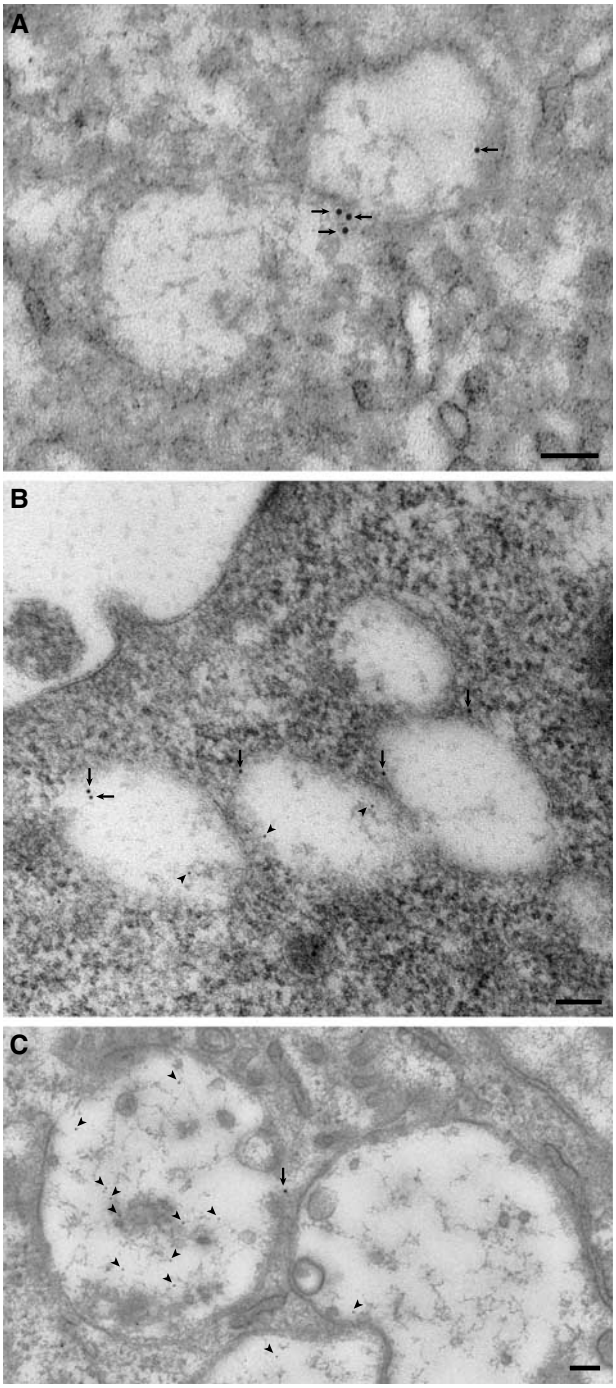

Figure 3 Double gold labeling immunoelectron microscopy of bone-resorbing osteoclasts. Arrows and arrowheads indicate VGLUT1 (10 nm in diameter) and bone degradation product (5 nm in diameter), respectively. (**A**) VGLUT1-containing small vesicles; (**B**) vesicles containing both VGLUT1 and bone degradation products localized near the basolateral region; (**C**) vesicles containing bone degradation products but little VGLUT1 localized near the ruffled border membrane. Bar = 100 nm.

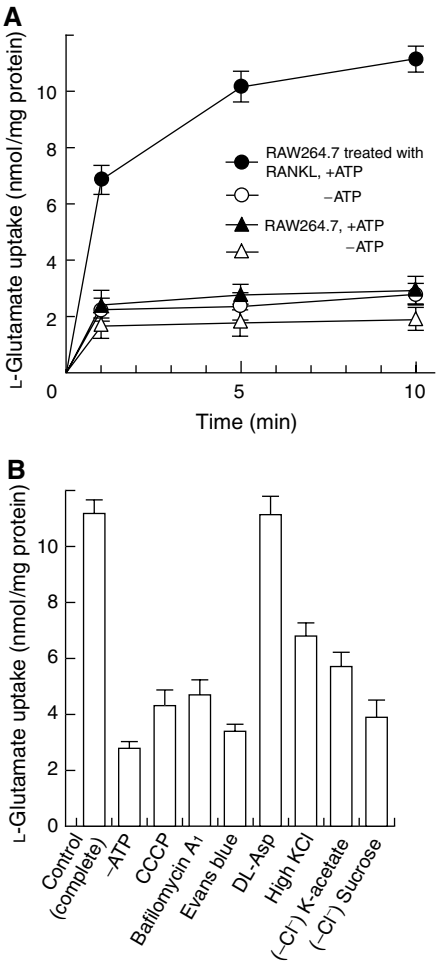

Figure 4 VGLUT1-mediated vesicular storage of L-glutamate. (**A**) Time course of L-glutamate uptake by membrane vesicles isolated from RAW264.7 cells treated with or without RANKL determined in the presence or absence of ATP; $n = 3$. (**B**) Effects of various compounds on the ATP-dependent L-glutamate uptake by membrane vesicles of RAW264.7 cells treated with RANKL for 1 week. Additions: bafilomycin A1, 1 μM; CCCP, 1 μM; Evans blue, 1 μM; D,L-aspartate, 10 mM; KCl, 100 mM. In some experiments, KCl was substituted with K-acetate or omitted from the assay medium. The results are shown as means ± s.e.m., $n = 4$.

Among known mGluRs, RT–PCR indicated the presence of mRNAs of mGluR3, mGluR4 and mGluR8 in RAW264.7 cells treated with RANKL and the presence of mGluR3, mGluR5 and mGluR8 in osteoclasts (Figure 7A and Supplementary Figure S3). Immunoreactivity for mGluR8 (Figure 7B) but not mGluR3 and mGluR4 was detected by immunohistochemical analysis in RAW264.7 cells treated with RANKL (data not shown), suggesting expression of mGluR8 in mature osteoclasts.

It is important to ask whether mGluR8 regulates transcytosis. Upon the addition of (1*S*,3*R*,4*S*)-1-aminocyclopentane-1,3,4-tricarboxylic acid (ACPT-I), a specific agonist of class III mGluRs (Acher *et al*, 1997), KCl-evoked secretions of both L-glutamate and bone degradation products decreased by about 90 and 87% of the control, respectively, and the inhibitions were blocked by the (*R*,*S*)-cyclopropyl-4-phosphonophenylglycine (CPPG), a specific antagonist (Toms *et al*, 1996), and dibutylylcAMP (DBcAMP), a non-hydrolyzable cAMP analogue (Figure 7C and D). Agonists for other mGluRs and NMDA receptor did not affect the secretions of L-glutamate (data not shown). mGluR8 is functionally coupled with the Gi protein, and thus its stimulation decreases intracellular cAMP content (Nakanishi, 1992). Consistent with these observations, both ACPT-I and L-glutamate decreased cAMP content, which were fully recovered by CPPG (Figure 7E).

These results are consistent with the idea that mGluR8 was functionally expressed in mature osteoclasts and inhibited transcytosis through an inhibitory cAMP cascade.

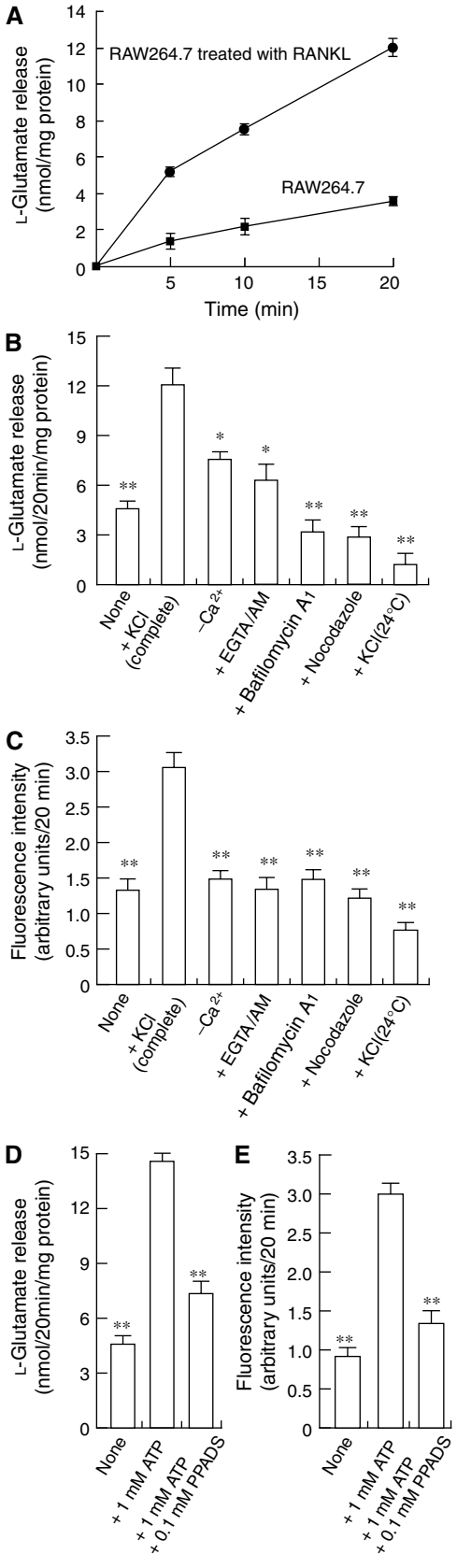

Blocking the glutamate signal stimulates the resorptive activity of osteoclasts

To reveal the physiological relevance of L-glutamate-mediated autoregulation of transcytosis, we investigated whether blocking the L-glutamate signaling with CPPG affects bone resorption. We monitored the area of bone resorption produced by osteoclasts on dentine slices as a functional marker for osteoclasts. α-MEM contains 0.5 mM L-glutamate, the concentration at which L-glutamate-mediated autosuppression of transcytosis may occur. Thus, under the culture conditions, CPPG stimulated the bone resorptive activity by 1.5-fold (Figure 8). Eel calcitonin at 10 nM inhibited bone resorption (Figure 8). These results suggest that blocking the glutamate signal stimulated bone resorptive activity by osteoclasts.

Finally, to determine whether preventing L-glutamate signaling causes phenotypic changes in the bone tissues, we assessed the bone mass of female VGLUT1$^{-/-}$ mice using microcomputed tomography. Comparing the bone masses in wild type and homozygotes, the bone mass, expressed as a ratio of BV/TV, of homozygotes had decreased and was significantly lower by the age of 4 months and exhibited osteoporosis-like symptoms (Figure 9). Essentially the same results were obtained in all homozygotes tested ($n=3$).

Discussion

The present results demonstrated that bone-resorbing osteoclasts were the site of L-glutamate signaling. Osteoclasts exhibited a glutamatergic phenotype upon maturation. Functional VGLUT1 was inducibly expressed in osteoclasts as demonstrated by molecular biological, biochemical and immunohistochemical techniques. VGLUT1 was associated with small clear vesicles and larger membrane vesicles that also contained bone degradation products (Figures 2 and 3). L-Glutamate and bone degradation products were secreted through transcytosis. L-Glutamate was not stored in vesicles of osteoclasts prepared from VGLUT1$^{-/-}$ mice. Consequently, osteoclasts prepared from VGLUT1$^{-/-}$ mice did not secrete L-glutamate. These results provided convincing evidence for the glutamatergic nature of osteoclasts.

Up until now, transcytosis of bone degradation products has been characterized primarily by morphological methods (Nesbitt and Horton, 1997; Salo *et al*, 1997; Mulari *et al*, 2003). Little is known about the mechanism of transcytosis. As some of VGLUT1 molecules were associated with trans-

Figure 5 Regulated secretion of L-glutamate and fluorescent bone degradation products from RAW264.7 cells treated with RANKL. (**A**) RAW264.7 cells treated with RANKL or RAW264.7 cells (2.0×10^5 cells/dish) were stimulated with 50 mM KCl. The L-glutamate released was measured. (**B**) L-Glutamate secretion after 20 min is shown. In some experiments, cells were treated for 2 h with 1 μM bafilomycin A1, 50 μM EGTA-AM or 10 μM nocodazole, and then stimulated with KCl. (**C**) Fluorescent bone degradation products in the medium under the conditions in panel B were assessed fluorometrically. The results are means±s.e.m., $n=4$. Asterisks indicate statistically significant numbers ($^*P<0.01$, $^{**}P<0.001$). ATP stimulates the secretion of L-glutamate (**D**) and fluorescent bone degradation products (**E**) from RAW264.7 cells treated with RANKL. The assay was started by the addition of 1 mM ATP. In some experiments, 0.1 mM PPADS was also included. The results are means±s.e.m., $n=4$. Asterisks indicate statistically significant numbers ($^*P<0.01$, $^{**}P<0.001$).

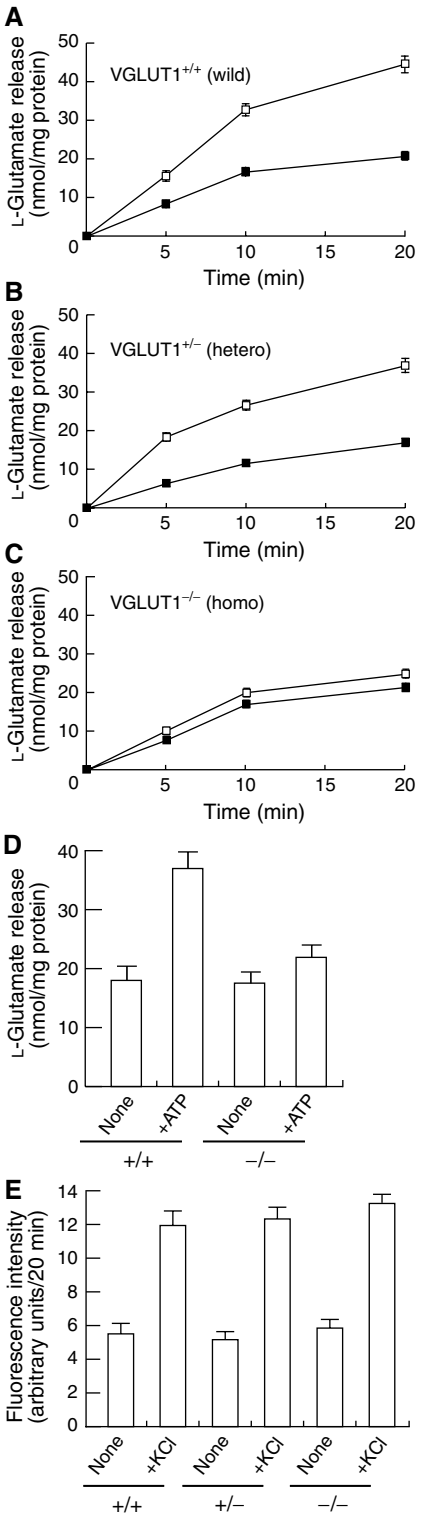

Figure 6 Both KCl- and ATP-dependent L-glutamate secretion were impaired in osteoclasts from VGLUT1$^{-/-}$ mice. The time course of KCl-dependent L-glutamate secretion from osteoclasts (2.0×10^5 cells/dish) prepared from bone marrow of wild-type VGLUT1$^{+/+}$ (**A**), VGLUT1$^{+/-}$ (**B**) or VGLUT1$^{-/-}$ (**C**) was measured as in Figure 5 in the presence (open squares) or absence (closed squares) of 50 mM KCl. (**D**) In osteoclasts (2.0×10^5 cells/dish) prepared from wild-type and VGLUT1$^{-/-}$ mice, L-glutamate secretion were measured 20 min after stimulation with 1 mM ATP. (**E**) Secretion of bone degradation products from osteoclasts under the conditions in panels A–C was assessed fluorometrically after 20 min. The results are means ± s.e.m., $n = 3$.

cytotic vesicles, we hypothesized that L-glutamate is co-localized and co-secreted with bone degradation products through transcytosis. Experiments were performed to characterize the secretion of L-glutamate and bone degradation products. The secretion of both was found to require, at least partially, the influx of extracellular Ca^{2+}. Moreover, inhibition of both secretory activities by a class III mGluR agonist, and the reversion of this effect with a specific antagonist suggested the requirement of cAMP for both secretion processes (Figure 7). Thus, secretion of L-glutamate and bone degradation products apparently involves regulated exocytotic processes that are similar to those in neurons and endocrine cells. In addition, both secretory activities showed similar temperature dependence and sensitivities to bafilomycin A1 and nocodazole. These results constitute evidence that L-glutamate and bone degradation products are secreted together through transcytosis. To our knowledge, this is the first direct evidence that transcytosis contains a regulated process. Presence of a regulated process in transcytosis suggests involvement of molecular machinery similar to that of the exocytotic pathway of neuronal synaptic vesicles and endocrine secretory granules. Identification of molecular components involved in the transcytosis such as soluble *N*-ethylmaleimide-sensitive attachment protein receptor (SNARE)-like proteins and voltage-gated Ca^{2+} channels in bone-resorbing osteoclasts is urgently needed for full characterization of the regulated transcytosis.

Another important feature of transcytosis is the involvement of an ionotropic purinergic P2 receptor(s) in the process. Osteoclasts as well as osteoblasts express multiple P2 receptor subtypes and an increasing amount of evidence has highlighted the importance of P2 receptors in the bone microenvironment and the bone remodeling processes (Gallagher and Buckley, 2002; Gartland *et al*, 2003). Which P2 subtype triggers secretion of L-glutamate and bone degradation products is unknown and awaits further study. As ATP is released from osteoblasts upon mechanical stimulation (Romanello *et al*, 2001; Jørgensen *et al*, 2002), our results suggest that osteoblasts affect transcytosis of osteoclasts through ATP and L-glutamate signaling pathways.

We propose the following secretory events during bone resorption: osteoclasts absorb bone degradation products through endocytosis and sequester them in transcytotic vesicles. Afterwards, VGLUT1-containing vesicles (small clear vesicles shown in Figure 3A) fuse with transcytotic vesicles and the resultant vesicles store both L-glutamate and bone degradation products (larger vesicles seen in Figure 3B). Subsequently, L-glutamate and other internal materials are secreted together through exocytosis (Figure 10, left panel). In osteoclasts of VGLUT1$^{-/-}$ mice, transcytotic vesicles apparently fused with vesicles containing no L-glutamate, which led to the secretion of bone degradation products without concomitant release of L-glutamate (Figure 10, right panel). Thus, the secretory pathways for L-glutamate and bone degradation products overlapped, but were not dependent upon one another. One can ask whether L-glutamate secretion is, at least in part, mediated through another secretory mechanism other than transcytosis, as the proportion of VGLUT1 associated with transcytotic vesicles is not known. This possibility seems to be unlikely, however, because the secretion of L-glutamate and bone degradation products shared similar biochemical and pharmacological characteris-

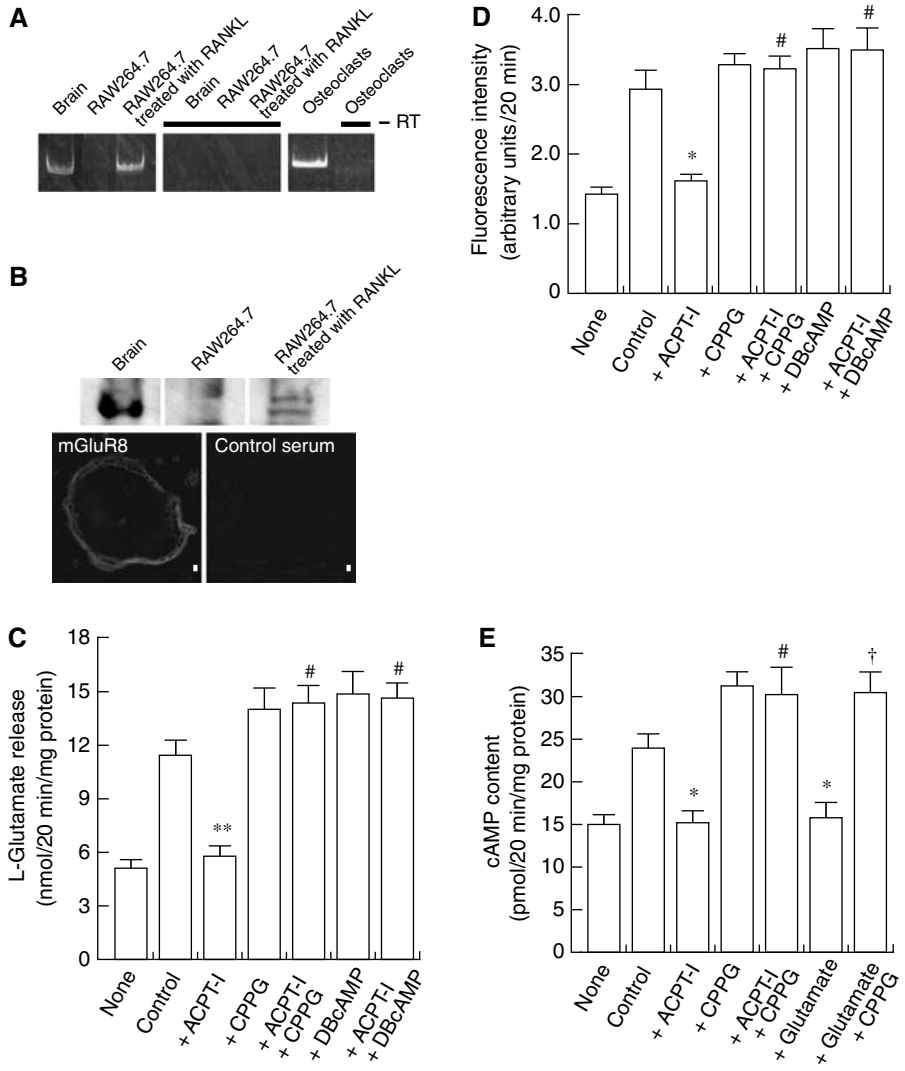

Figure 7 mGluR-mediated regulation of the secretion of L-glutamate and fluorescent bone degradation products from RAW264.7 cells treated with RANKL. (**A**) Expression of mGluR8 gene as revealed by RT–PCR. (**B**) Expression of mGluR8 as revealed by immunoblotting (upper panel) and immunohistochemistry (lower panel). Bar = 10 μm. (**C**) RAW264.7 cells treated with RANKL (2.0×10^5 cells/dish) were incubated in the presence or absence of agonists or antagonists of glutamate receptors or DBcAMP as indicated and then stimulated with 50 mM KCl. The L-glutamate released after 20 min is shown. The results are means ± s.e.m., $n = 3$. Asterisks and marks indicate statistically significant numbers (**$P < 0.001$ compared with control, $^{\#}P < 0.001$ compared with + ACPT-I). (**D**) Fluorescent bone degradation products in the medium under the conditions in panel A were assessed fluorometrically. The results are means ± s.e.m., $n = 3$. Asterisks and marks indicate statistically significant numbers (*$P < 0.01$ compared with control, $^{\#}P < 0.001$ compared with + ACPT-I). (**E**) cAMP content in the osteoclast-like cells (2.0×10^5 cells/dish) under the conditions in panel A was measured. The results are means ± s.e.m., $n = 3$. Asterisks and marks indicate statistically significant numbers (*$P < 0.01$ compared with control, $^{\#}P < 0.001$ compared with + ACPT-I, $^{\dagger}P < 0.001$, compared with + L-glutamate). Additions: L-glutamate, 0.5 mM; ACPT-I, 50 μM; CPPG, 100 μM; DBcAMP, 1 mM.

tics as described above. More detailed and quantitative study will clarify this issue. In any event, transcytosis of L-glutamate and bone degradation products appears to be a more complex secretory event than previously thought.

We have provided evidence that L-glutamate and bone degradation products were secreted through transcytosis. Through this, L-glutamate may act in a paracrine/autocrine manner, allowing regulation of cellular function and/or differentiation by way of glutamate receptors (Mason, 2004). In our studies, we found that mGluR8 decreased cAMP content and inhibited KCl-evoked secretion of L-glutamate and bone degradation products. Thus, L-glutamate secreted through transcytosis may be involved in the negative feedback cascade for transcytosis (Figure 10). This is reminiscent of L-glutamate signaling in pineal glands (Yamada *et al*, 1998) and islet of Langerhans (Uehara *et al*, 2004) that leads to the inhibition of melatonin synthesis and glucagon secretion by way of mGluR2/3 and mGluR4, respectively. mGluR-coupled autoregulation may be a common feature of L-glutamate signaling in the peripheral tissue.

One of the significant findings in the present study is that VGLUT1$^{-/-}$ mice develop osteoporosis 4 months after birth (Figure 9). As glutamate signaling may involve a negative feedback regulation of transcytosis as described above, under normal physiological conditions, bone resorption should be suppressed by L-glutamate signaling. The fact that blocking the L-glutamate-mediated autoregulatory cascade by an mGluR8 antagonist enhanced bone resorption supports this

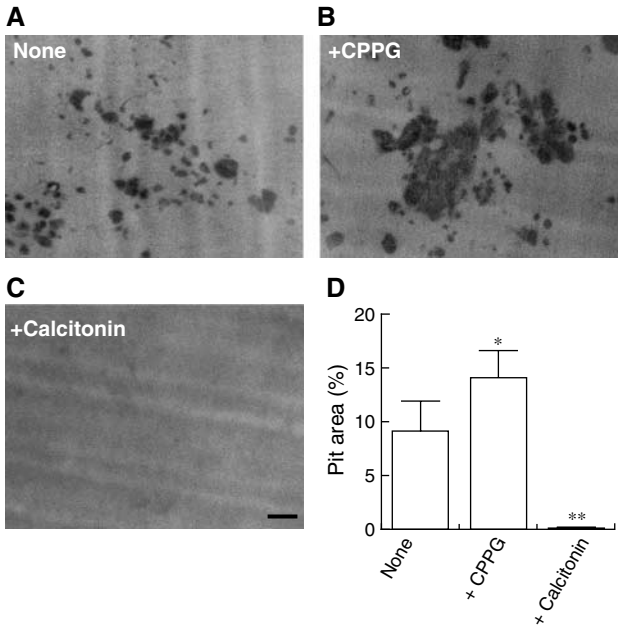

Figure 8 Inhibition of L-glutamate signal stimulated bone resorptive activity. Osteoclasts were cultured on dentine slices in the absence (**A**) or presence (**B**) of 100 μM CPPG. In some experiments, 10 nM eel calcitonin was added (**C**). After 24 h, the resorption pits formed on the dentine slices were stained with Mayer's hematoxylin and quantified using the NIH Image program. The pictures of typical resorption pits formed on the dentine slices under respective conditions are shown. (**D**) Ratio of resorption area to total area (pit area expressed in %) is shown. $*P<0.01$, $**P<0.001$ compared with control. The results are means ± s.e.m., $n=6$. Bar = 100 μm.

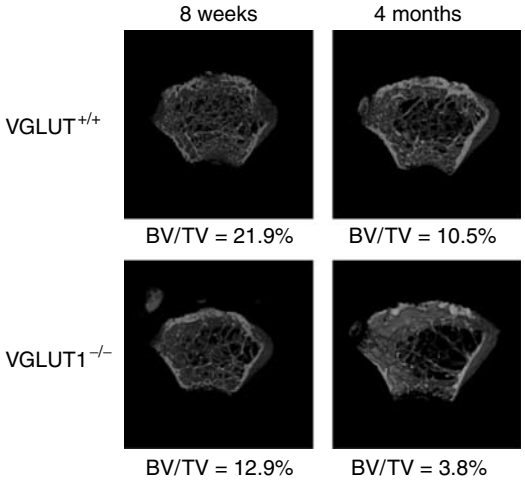

Figure 9 Microcomputed tomographs of female mouse femora from VGLUT1$^{+/+}$ and VGLUT1$^{-/-}$ mice. Microcomputed tomography 3D images of femoral metaphyses of VGLUT1$^{+/+}$ and VGLUT1$^{-/-}$ at the ages of 8 weeks (left) and 4 months (right) were constructed. The values of BV/TV are shown under each picture.

idea (Figure 8). In osteoclasts of VGLUT1$^{-/-}$ mice, the loss of the ability to secrete L-glutamate did not affect secretion of bone degradation products (Figure 6E). Thus, the negative feedback regulation in osteoclasts is impaired in VGLUT1$^{-/-}$ mice, leaving the osteoclasts in a desuppressed state that led to elevated bone resorption that, in turn, led to osteoporosis (Figure 10, right panel). As purinergic stimulation facilitates L-glutamate secretion (Figure 5), it is expected that inhibition of purinergic signaling causes similar effects on osteoclastic activity. In this respect, it is noteworthy that deletion of the ionotropic P2X7 receptor causes increased trabecular bone resorption (Ke *et al*, 2003). To our knowledge, this is the first report presenting direct evidence that impairment of glutamate signaling is associated with a metabolic disorder. Further studies, especially quantitative analyses as to interrelationship among glutamate signaling, transcytosis of bone degradation products and bone digestion, are necessary to elucidate the detailed signaling cascade and how impairment of glutamate signaling leads to osteoporosis.

The finding that transcytotic vesicles serve as storage organelles for L-glutamate expands the concept of the glutamate signaling. In addition to neuronal synaptic vesicles, we have shown that VGLUTs are functionally associated with synaptic-like microvesicles in pinealocytes, hormone-containing secretory granules in islet α and F cells and intestinal L cells, and acrosomes of early spermatid (Moriyama and Yamamoto, 2004; Uehara *et al*, 2006). Transcytotic vesicles are the fifth organelles to show vesicular storage of L-glutamate. Transcytotic vesicles are morphologically and biochemically distinct from known secretory vesicles. Further characterization of transcytotic vesicles as L-glutamate storage organelles, such as the intravesicular concentration of L-glutamate, pH and the kinetics of L-glutamate secretion, is important to reveal the common aspects and diversity in L-glutamate signaling.

In conclusion, we have clarified the issues of when, where and how L-glutamate is secreted in bone tissues. Glutamatergic signal transmission may play essential regulatory role(s) in bone homeostasis, as impairment of L-glutamate signaling stimulates bone resorptive activity, leading to osteoporosis.

Materials and methods

Cell cultures

Primary osteoblasts were prepared from newborn ddY mice by sequential enzymatic digestion as previously described (Suda *et al*, 1997). Osteoclasts were induced to differentiate into mature osteoclasts by the co-culture method described by Suda *et al* (1997) with slight modifications. More than 90% of the adherent cells were TRAP-positive, which were used for experiments after prolonged incubation. To differentiate osteoclasts from RAW264.7 cells, the cells were treated with 100 ng/ml extracellular domain of RANKL (sRANKL) (Peprotech EC) and 10 000 U/ml macrophage colony-stimulating factor (Kyowa Hakko) as described (Toyomura *et al*, 2003). Primary osteoblasts and clonal bone cell lines including MC3T3-E1, MC3T3-G2/PA6, ST2 (Udagawa *et al*, 1989) and C3H10T1/2 (Levine and Teegarden, 2004) were cultured as described.

VGLUT1 knockout (−/−) mice

A line of VGLUT1$^{-/-}$ mice was maintained as heterozygotes by continuous backcrossing with wild-type$^{+/+}$ C57/BL6 mice, as described (Fremeau *et al*, 2004b). Mice were genotyped by PCR (Fremeau *et al*, 2004b) before use.

RT–PCR and Northern analysis

Total RNA (1 μg) extracted from cultured cells was transcribed into cDNA in a final volume of 20 μl of a reaction buffer containing 0.2 mM each dNTP, 10 mM dithiothreitol, 100 pmol of random octamers and 200 U of Moloney murine leukemia virus reverse transcriptase (Amersham). After 1 h incubation at 42°C, the reaction was terminated by heating at 90°C for 5 min. The PCR

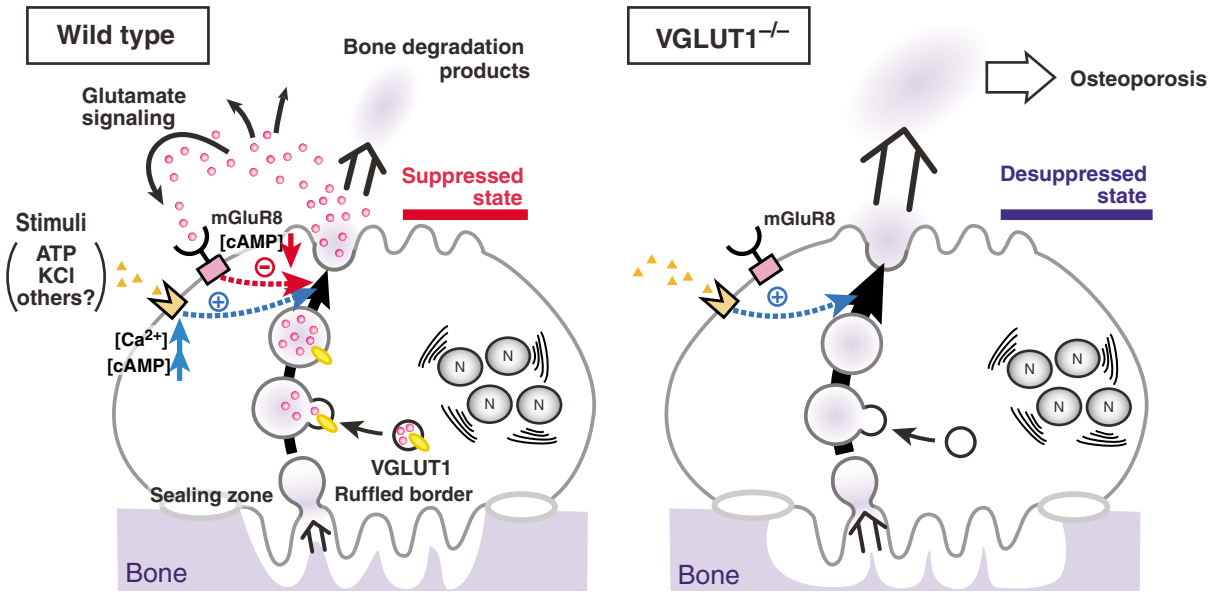

Figure 10 Proposed L-glutamate signaling during bone resorption. (left) Under the normal physiological conditions, a proportion of VGLUT1-containing small clear vesicles may fuse with the transcytotic vesicle. Upon stimulation with KCl or ATP, L-glutamate and bone degradation products are secreted through transcytosis. Then, the released L-glutamate acts as a negative feedback regulator through mGluR8-mediated signaling pathway, keeping osteoclasts in the suppressed state. (right) In osteoclasts of VGLUT1$^{-/-}$ mice, L-glutamate-mediated signaling pathway is impaired. This may induce the desuppressive state of osteoclasts, causing stimulated bone resorption followed by osteoporosis. N, nucleus.

amplification was performed as described (Hayashi *et al*, 2003a). The sequences of the oligonucleotides used as primers were based on the published sequences, and are shown in Supplementary Table SI. DNA sequencing was performed by the chain termination method. For Northern blotting, the mRNA (4.5 μg per lane) was separated on a 1% agarose gel containing formaldehyde and then transferred to a nylon membrane (Amersham). The immobilized RNA was probed with cDNA fragments of VGLUT (nt 270–706) labeled with [^{32}P]dCTP (3000 Ci/mmol; Amersham) by random priming. After extensive washing, the membrane was subjected to autoradiography using BAS 1000 film (Fuji Film Co.).

Antibodies

Site-specific polyclonal antibodies against rat VGLUT1, V-ATPase subunit A and mGluR4 were prepared; their immunological specificities have been described elsewhere (Hayashi *et al*, 2003b; Uehara *et al*, 2004). Guinea-pig polyclonal antibodies against mGluR8 and rabbit polyclonal antibodies against mGluR2/3 were purchased from Chemicon. The following antibodies were used as organelle markers: mouse monoclonal antibody 6C4 (kindly supplied by Dr T Kobayashi, Riken, Wako, Japan); mouse monoclonal antibodies against α-tubulin (Sigma), TfR (NeoMarkers), cathepsin K (Oncogene Research Products), TGN38 (Transduction Laboratories) and GM130 (BD Transduction Laboratories); rat monoclonal antibodies against lamp2 (Developmental Studies Hybridoma Bank). Alexa Fluor 488-labeled anti-rabbit IgG, Alexa Fluor 568-labeled anti-mouse IgG and Alexa Fluor 568-labeled phalloidin were obtained from Molecular Probes and IgG conjugated with colloidal gold from British Biocell International Ltd.

Western blotting

Membrane fractions from RAW264.7 cells treated with RANKL or untreated cells (1×10^8 cells each) were prepared and denatured with SDS sample buffer containing 1% SDS and 10% β-mercaptoethanol. Then, Western analysis was performed as described by Hayashi *et al*. (2003a).

Immunohistochemistry

The procedure of Hayashi *et al*. (2003a, b) was used. In brief, cells on collagen-coated coverslips were fixed with 4% paraformaldehyde in PBS for 30 min, followed by a 15 min incubation in PBS containing 0.1% Triton X-100, 2% goat serum and 1% bovine serum albumin (BSA), and finally reacted with antibodies at 1 μg/ml or diluted 1000-fold (anti-VGLUT1 or other antibody) in PBS containing 0.5% BSA for 1 h at room temperature. Samples were washed four times with PBS and then reacted with the secondary antibody for 1 h at room temperature. The secondary antibodies used were Alexa Fluor 568-labeled anti-mouse IgG (1 μg/ml) or Alexa Fluor 488-labeled anti-rabbit IgG (2 μg/ml) (Molecular Probes). Finally, the immunoreactivity was examined under an Olympus FV300 confocal laser microscope.

For immunostaining of femur sections, mice were anesthetized with ether and then perfused intracardially with saline, followed by 4% paraformaldehyde in 0.1 M phosphate buffer (pH 7.4). The femora were isolated and immersed in the same solution overnight at 4°C. After washing with PBS, the femora were decalcified with 9% EDTA-2Na and 10% EDTA-4Na in PBS at 4°C for 1 week. They were successively infiltrated with 30% sucrose in PBS, embedded in OTC compound (Sakura Finetek), sectioned at a thickness of 6 μm and then mounted on gelatin-coated slides. The immunological reaction was performed as described above. Histochemical staining for TRAP with HRP-DAB was performed as described (Nakamura *et al*, 1994).

Immunoelectron microscopy

Samples were fixed with 0.2% glutaraldehyde and 4% paraformaldehyde in 0.1 M phosphate buffer (pH 7.4), dehydrated and then embedded in LR white for 2 days at −20°C. Ultrathin sections on nickel grids were incubated with PBS containing 2% goat serum and 2% BSA for 10 min, followed by incubation with a mixture of rabbit anti-VGLUT1 antiserum (diluted 50-fold) and mouse anti-FITC monoclonal antibodies (diluted 125-fold) for 1 h at room temperature and, finally, incubation with a mixture of secondary antibodies conjugated with colloidal gold for 15 min at room temperature (Hayashi *et al*, 2003a). After washing with 0.1 M sodium cacodylate buffer (pH 7.4), the sections were postfixed in 5% glutaraldehyde in the cacodylate buffer, stained sequentially with uranyl acetate for 10 min and lead citrate for 1 min, and observed under a Hitachi H-7100S electron microscope.

L-Glutamate uptake

A membrane fraction of cultured cells was prepared as described above and used for the transport assay within a day of preparation; the samples were not frozen. L-Glutamate uptake by membrane vesicles was measured as described in the solution comprising membranes (0.1 mg protein), 20 mM MOPS–Tris (pH 7.0), 5 mM

Mg-acetate, 4 mM KCl, 0.3 M sucrose and 100 μM [^{3}H]-L-glutamate in the presence or absence of ATP (Tris salt) at 30°C (Moriyama and Yamamoto, 1995).

Secretion of L-glutamate and fluorescent bone degradation products

RAW-derived osteoclast-like cells or osteoclasts (2.0×10^5 cells/dish) were washed three times with Ringer's solution and then incubated for 30 min at 37°C. The cells were incubated in Ringer's solution and stimulated by the addition of either 50 mM KCl or 1 mM ATP (final concentrations). When necessary, agonists or antagonists of glutamate receptors, obtained from Tocris Cookson (Avonmouth, UK), at the indicated concentrations were included. At the times indicated, samples (100 μl) were carefully taken and the amount of L-glutamate was determined by HPLC with a RESOLVE C18 column (4.6 mm × 150 mm; Waters Ltd) and fluorescence detection as described previously (Hayashi *et al*, 2003a). To measure secretion of bone degradation products, osteoclasts (1.0×10^3 cells) were cultured on dentine disks, which were labeled with the seminaphthofluorescein dye 5,6-carboxyl-SNAFL®-2 (Molecular Probes) as described by Stenbeck and Horton (2004). After incubation for 12 h, the osteoclasts were stimulated by the addition of either 50 mM KCl or 1 mM ATP (final concentrations). Then, 100 μl medium was carefully sampled and diluted with 1.9 ml glycine–NaOH (pH 10.0) and the fluorescence intensity measured.

Measurement of cAMP

cAMP was quantified with the enzyme immunoassay kit obtained from Cayman Chemical (Ann Arbor, MI), according to the manufacturer's manual.

Measurement of bone resorption activity

The resorption pit assay was performed as described by Li *et al* (2002). Co-cultured osteoclasts on collagen gel-coated dishes were detached with 0.2% collagenase and plated on dentine slices and cultured in α-MEM medium containing 10% FBS in the presence or absence of 100 μM CPPG for 24 h. In control experiments, eel calcitonin (Elcatonin, Asahi Chemical Industry Co., Tokyo) at 10 nM was included. Resorption pits on the dentine slices were visualized by staining with Mayer's hematoxylin, and observed under an Olympus BX60 microscope. To quantify the resorption areas, five areas of dentine slices were randomly selected and stained resorption lacunae were measured with NIH Image program.

Bone morphometry

To assess the parameters for bone morphometry, 8-week and 4-month-old VGLUT1$^{+/+}$ and VGLUT1$^{-/-}$ mice were anesthetized with ether and perfused intracardially with saline, followed by 4% paraformaldehyde in 0.1 M phosphate buffer (pH 7.4). The femora were then isolated and immersed in 4% paraformaldehyde in PBS at 4°C. The images were taken by micro-focus X-ray computed tomography (ScanXmate-A080, COMSCAN TECNO CO. Ltd) and reconstituted into 3D images with Fan CT. The ratio of trabecular bone volume to total tissue volume (BV/TV) was calculated with analytic software (TRI/3D BON, Ratoc System Engineering Co. Ltd) (Sone *et al*, 2004). The trabecular bone in the distal metaphysis of the femur was chosen as the sampling site, which was located from 0.5 to 1.5 mm from the growth plate.

Data analysis

All numerical values are shown as means ± s.e.m. (standard error of the mean). n is the number of experiments. The significance of differences between the mean values of two indicated groups was evaluated with the Student's t-test. Statistical evaluations were performed using MS Excel (version 11.0).

Supplementary data

Supplementary data are available at *The EMBO Journal* Online (http://www.embojournal.org).

Acknowledgements

We thank Professor Naoyuki Takahashi for discussion and Misses Miki Hiasa and Kahori Shimizu for their help with immunohistochemistry. RM, MH and SY were supported by Research Fellowships from the Japan Society for the Promotion of Science for Young Scientists. This work was supported in part by Japanese Ministry of Education, Science, Sport, and Culture Grant-in Aid for Research 18390026 and 18050025 to YM and 15079208 to AY.

References

Acher FC, Tellier FJ, Azerad R, Brabet IN, Fagni L, Pin JP (1997) Synthesis and pharmacological characterization of aminocyclopentanetricarboxylic acids: new tools to discriminate between metabotropic glutamate receptor subtypes. *J Med Chem* **40:** 3119–3129

Baron R, Bartkiewicz M, David P, Hernando-Sobrino N (1994) Acidification and bone resorption: the role and characteristics of V-ATPases in the osteoclast. In *Molecular Biology Intelligence Unit. Organellar Proton-ATPases*, Nelson N (ed) pp 49–73. Springer-Verlag: RG Landes Company

Bhangu PS, Genever PG, Spencer GJ, Grewal TS, Skerry TM (2001) Evidence for targeted vesicular glutamate exocytosis in osteoblasts. *Bone* **29:** 16–23

Blair HC (1998) How the osteoclast degrades bone. *BioEssays* **20:** 837–846

Bowman EJ, Siebers A, Altendorf K (1988) Bafilomycins: a class of inhibitors of membrane ATPases from microorganisms, animal cells, and plant cells. *Proc Natl Acad Sci USA* **85:** 7972–7976

Boyle WJ, Simonet WS, Lacey DL (2003) Osteoclast differentiation and activation. *Nature* **423:** 337–342

Eriksen EF (1986) Normal and pathological remodeling of human trabecular bone: three dimensional reconstruction of the remodeling sequence in normal and in metabolic bone disease. *Endocr Rev* **7:** 379–408

Fremeau Jr RT, Kam K, Qureshi T, Johnson J, Copenhagen DR, Storm-Mathisen J, Chaudhry FA, Nicoll RA, Edwards RH (2004b) Vesicular glutamate transporters 1 and 2 target to functionally distinct synaptic release sites. *Science* **304:** 1815–1819

Fremeau Jr RT, Voglmaier S, Seal RP, Edwards RH (2004a) VGLUTs define subsets of excitatory neurons and suggest novel roles for glutamate. *Trends Neurosci* **27:** 98–103

Gallagher JA, Buckley KA (2002) Expression and function of P2 receptors in bone. *J Musculoskel Neuron Interact* **2:** 432–439

Gartland A, Buckley KA, Hipskind RA, Bowler WB, Gallagher JA (2003) P2 receptors in bone-modulation of osteoclast formation and activity via P2X7 activation. *Crit Rev Eukaryot Gene Expr* **13:** 237–242

Hayashi M, Morimoto R, Yamamoto A, Moriyama Y (2003a) Expression and localization of vesicular glutamate transporters in pancreatic islets, upper gastrointestinal tract, and testis. *J Histochem Cytochem* **51:** 1375–1390

Hayashi M, Yamada H, Uehara S, Morimoto R, Muroyama A, Yatsushiro S, Takeda J, Yamamoto A, Moriyama Y (2003b) Secretory granule-mediated co-secretion of L-glutamate and glucagon triggers glutamatergic signal transmission in islets of Langerhans. *J Biol Chem* **278:** 1966–1974

Hinoi E, Fujimori S, Nakamura Y, Yoneda Y (2001) Group III metabotropic glutamate receptors in rat cultured calvarial osteoblasts. *Biochem Biophys Res Commun* **281:** 341–346

Hinoi E, Fujimori S, Takarada T, Taniura H, Yoneda Y (2002) Facilitation of glutamate release by ionotropic glutamate receptors in osteoblasts. *Biochem Biophys Res Commun* **297:** 452–458

Jørgensen NR, Henriksen Z, Sørensen OH, Eriksen EF, Civitelli R, Steinberg TH (2002) Intercellular calcium signaling occurs between human osteoblasts and osteoclasts and requires activation of osteoclast P2X7 receptors. *J Biol Chem* **277:** 7574–7580

Kajiya H, Okamoto F, Fukushima H, Takada K, Okabe K (2003) Mechanism and role of high-potassium-induced reduction of intracellular Ca^{2+} concentration in rat osteoclasts. *Am J Physiol Cell Physiol* **285:** C457–C466

Ke HZ, Qi H, Weidema F, Zhang Q, Panupinthu N, Crawford DT, Grasser WA, Paralkar VM, Li M, Audoly LP, Gabel CA, Jee WSS, Dixon SJ, Sims AM, Thompson DD (2003) Deletion of the P2X7

nucleotide receptor reveals its regulatory roles in bone formation and resorption. *Mol Endocrinol* **17:** 1356–1367

Levine MJ, Teegarden D (2004) 1α,25-dihydroxycholecalciferol increases the expression of vascular endothelial growth factor in C3H10T1/2 mouse embryo fibroblasts. *J Nutr* **134:** 2244–2250

Li X, Udagawa N, Itoh K, Suda K, Murase Y, Nishihara T, Suda T, Takahashi N (2002) p38 MAPK-mediated signals are required for inducing osteoclast differentiation but not for osteoclast function. *Endocrinology* **143:** 3105–3113

Mason DJ (2004) Glutamate signaling and its potential application to tissue engineering of bone. *Eur Cell Mater* **7:** 12–25

Maycox PR, Hell JW, Jahn R (1990) Amino acid neurotransmission: spotlight on synaptic vesicles. *Trends Neurosci* **13:** 83–87

Moriyama Y, Yamamoto A (1995) Vesicular glutamate transporter in microvesicles from bovine pineal glands: driving force, mechanism of chloride anion activation, and substrate specificity. *J Biol Chem* **270:** 22314–22320

Moriyama Y, Yamamoto A (2004) Glutamatergic chemical transmission: look! Here, there, and anywhere. *J Biochem* **135:** 155–163

Mulari M, Vääräniemi J, Väänänen HK (2003) Intracellular membrane trafficking in bone resorbing osteoclasts. *Microsc Res Tech* **61:** 496–503

Naemsch LN, Dixon SJ, Sims SM (2001) Activity-dependent development of $P2X_7$ current and Ca^{2+} entry in rabbit osteoclasts. *J Biol Chem* **276:** 39107–39114

Nakamura H, Moriyama Y, Futai M, Ozawa H (1994) Immunohistochemical localization of vacuolar H^+-ATPase in osteoclasts of rat tibiae. *Arch Histol Cytol* **57:** 535–539

Nakanishi S (1992) Molecular diversity of glutamate receptors and implications for brain function. *Science* **258:** 597–603

Nesbitt SA, Horton MA (1997) Trafficking of matrix collagens through bone-resorbing osteoclasts. *Science* **276:** 266–269

Palokangas H, Mulari M, Väänänen HK (1997) Endocytic pathway from the basal plasma membrane to the ruffled border membrane in bone-resorbing osteoclasts. *J Cell Sci* **110:** 1767–1780

Ralevic V, Burnstock G (1998) Receptors for purines and pyrimidines. *Pharmacol Rev* **50:** 413–492

Rodan GA, Martin TJ (2000) Therapeutic approaches to bone diseases. *Science* **289:** 1508–1514

Romanello M, Pani B, Bicego M, D'Andrea P (2001) Mechanically induced ATP release from human osteoblastic cells. *Biochem Biophys Res Commun* **289:** 1275–1281

Roseth S, Fykse EM, Fonnum F (1998) Uptake of L-glutamate into synaptic vesicles: competitive inhibition by dyes with biphenyl and amino- and sulphonic acid-substituted naphthyl groups. *Biochem Pharmacol* **56:** 1243–1249

Salo J, Lehenkari P, Mulari M, Metsikkö K, Väänänen HK (1997) Removal of osteoclast bone resorption products by transcytosis. *Science* **276:** 270–273

Serre CM, Farlay D, Delmas PD, Chenu C (1999) Evidence for a dense and intimate innervation of the bone tissue, including glutamate-containing fibers. *Bone* **25:** 623–629

Skerry TM, Taylor AF (2001) Glutamate signaling in bone. *Curr Pharm Des* **7:** 737–750

Sone T, Tamada T, Jo Y, Miyoshi H, Fukunaga M (2004) Analysis of three-dimensional microarchitecture and degree of mineralization in bone metastases from prostate cancer using synchrotron microcomputed tomography. *Bone* **35:** 432–438

Stenbeck G, Horton MA (2004) Endocytic trafficking in actively resorbing osteoclasts. *J Cell Sci* **117:** 827–836

Suda T, Jimi E, Nakamura I, Takahashi N (1997) Role of 1α,25-dihydroxyvitamin D_3 in osteoclast differentiation and function. *Methods Enzymol* **282:** 223–235

Toms NJ, Jane DE, Kemp MC, Bedingfield JS, Roberts PJ (1996) The effects of (*RS*)-α-cyclopropyl-4-phosphonophenylglycine ((RS)-CPPG), a potent and selective metabotropic glutamate receptor antagonist. *Br J Pharmacol* **119:** 851–854

Toyomura T, Murata Y, Yamamoto A, Oka T, Sun-Wada GH, Wada Y, Futai M (2003) From lysosomes to the plasma membrane. Localization of vacuolar type H^+-ATPase with the a3 isoform during osteoclast differentiation. *J Biol Chem* **278:** 22023–22030

Udagawa N, Takahashi N, Akatsu T, Sasaki T, Yamaguchi A, Kodama H, Martin TJ, Suda T (1989) The bone marrow-derived stromal cell lines MC3T3-G2/PA6 and ST2 support osteoclast-like cell differentiation in cocultures with mouse spleen cells. *Endocrinology* **125:** 1805–1813

Uehara S, Jung S-K, Morimoto R, Arioka S, Miyaji T, Juge N, Hiasa M, Shimizu K, Ishimura A, Otsuka M, Yamamoto A, Maechler P, Moriyama Y (2006) Vesicular storage and secretion of L-glutamate from glucagon-like peptide 1-secreting clonal intestinal L cells. *J Neurochem* **96:** 550–560

Uehara S, Muroyama A, Echigo N, Morimoto R, Otsuka M, Yatsushiro S, Moriyama Y (2004) Metabotropic glutamate receptor type 4 is involved in autoinhibitory cascade for glucagon secretion by α cells of islet of Langerhans. *Diabetes* **53:** 998–1006

Väänänen HK, Zhao H, Mulari M, Halleen JM (2000) The cell biology of osteoclast function. *J Cell Sci* **113:** 377–381

Vääräniemi J, Halleen JM, Kaarlonen K, Ylipahkala H, Alatalo SL, Andersson G, Kaija H, Vihko P, Väänänen HK (2004) Intracellular machinery for matrix degradation in bone-resorbing osteoclasts. *J Bone Miner Res* **19:** 1432–1440

Yamada H, Yatsushiro S, Ishio S, Hayashi M, Nishi T, Yamamoto A, Futai M, Yamaguchi A, Moriyama Y (1998) Metabotropic glutamate receptors negatively regulate melatonin synthesis in rat pinealocytes. *J Neurosci* **18:** 2056–2062

